Relaxation of Spherical Micellar Systems of Styrene−Isoprene Diblock Copolymers. 1. Linear Viscoelastic and Dielectric Behavior

Tomohiro Sato, Hiroshi Watanabe,* and Kunihiro Osaki

Institute for Chemical Research, Kyoto University, Uji, Kyoto 611, Japan

Ming-Long Yao

Rheometric Scientific F. E., 2-19-6 Yanagibashi, Taito-ku, Tokyo 111, Japan

Received December 14, 1995; Revised Manuscript Received March 4, 1996[⊗]

ABSTRACT: Linear viscoelastic and dielectric relaxation behavior was examined for blends of styrene−isoprene (SI) diblock copolymers in a nonentangling homopolyisoprene (hI) matrix. The copolymers formed spherical micelles with S cores and I corona. The I blocks had type-A dipoles, and their global motion induced dielectric relaxation. The micelles exhibited fast and slow relaxation processes for both dielectric loss ϵ'' and viscoelastic moduli G*. *For the fast process*, a nearly universal relationship was found for reduced moduli $G_r^* = [M_{bI}/c_{bI}RT]G^*_{SI}$ and reduced frequencies $\omega\tau^*$, where G^*_{SI} was the contribution of the SI micelles to G^*, M_{bI} and c_{bI} were the molecular weight and concentration for the I block, and τ^* was a relaxation time that increased *exponentially* with c_{bI} for large c_{bI}. Similar behavior was found also for ϵ''_{SI} (SI contribution to ϵ''). These features were qualitatively the same as those for the relaxation of star chains, indicating that the fast process corresponded to starlike relaxation of individual I blocks tethered on the S cores. Effects of the S cores on τ^* were discussed within the content of the tube model. *For the slow process of the concentrated micelles entangled through their I blocks*, a relaxation time τ_s was close to the Stokes−Einstein (SE) diffusion time τ_{SE} evaluated from the viscosity associated with the fast process. Thus, the slow process of those concentrated micelles was attributed to their SE diffusion governed by the relaxation of individual corona I blocks. On the other hand, for dilute micelles in the nonentangling matrix, τ_s was significantly shorter than τ_{SE} but close to the SE diffusion time evaluated from the matrix viscosity. This result suggested that the slow process of those micelles corresponded to the SE diffusion in the pure matrix.

I. Introduction

Rheology of block copolymers is strongly influenced by microdomain structures. More than ten years ago, Watanabe and co-workers[1−4] carried out systematic studies for rheology of moderately concentrated solutions of styrene−butadiene (SB) diblock copolymers in a low molecular weight B-selective solvent, *n*-tetradecane (C_{14}). They found the following features.[1−4] The solutions containing micelles with glassy S cores and solvated B corona exhibit elastic responses and do not relax (or flow) against sufficiently small, slow strains while the solutions flow against large strains. This *plastic* behavior emerges due to cubic lattices of the micelles having a typical lattice spacing of ≅400−900 Å.[1,2] This lattice, referred to as a macrolattice, is formed due to the balance of contradicting thermodynamic requirements for the corona B blocks, an osmotic requirement of uniform concentration distribution in the corona phase and an elastic requirement of randomized block conformation.[1−4] In fact, in a polymeric B-selective solvent, homopolybutadiene (hB), the macrolattice is disordered and the micelles are randomly dispersed to exhibit no plasticity unless the SB micelle content is very large:[4] The hB molecules screen the osmotic requirement for the corona B blocks, thereby allowing the B blocks to take a randomized conformation without violating the osmotic requirement.

Those SB/hB micellar blends containing no macrolattice exhibit viscoelastic relaxation.[4] However, differing from homopolymer systems, the blends exhibit extraordinarily slow, terminal relaxation processes.[5−7] Watanabe and co-workers[5−7] attributed those processes to diffusion of the SB micelles, but they did not specify a molecular origin of faster relaxation processes that were also detected in their experiments. Recently, we re-analyzed their data and examined the origin of the fast process.[8] The analysis suggested that the fast process corresponds to relaxation of individual corona B blocks tethered on the S cores. However, the analysis was limited to the linear viscoelastic data for the SB/hB micellar blends, and further studies were desired for both fast and slow relaxation processes of the micelles.

In those studies, it is interesting to examine dielectric behavior of micelles having type-A dipoles[9] in their corona blocks. The type-A dipoles parallel along the chain contour enable us to dielectrically observe global relaxation of the blocks.[10−13] It is also interesting and informative to examine nonlinear stress relaxation behavior of the micellar blends. Nonlinear relaxation data accumulated for homopolymer systems[14−17] are expected to be useful for specifying the fast and slow relaxation mechanisms of the blends. Styrene−isoprene (SI) diblock copolymers have type-A dipoles in the I blocks. Thus, their micellar blends in homopolyisoprene (hI) matrices are convenient model systems for extensive studies of the fast and slow processes.

From these points of view, we have carried out dielectric, linear viscoelastic, and nonlinear stress relaxation experiments for SI/hI micellar blends. This paper (part 1) examines linear viscoelastic and dielectric behavior and discusses molecular mechanisms for the fast and slow processes at equilibrium, placing emphasis on the difference between those processes. The accompanying paper (part 2) examines nonlinear stress relaxation behavior and demonstrates characteristic

[⊗] Abstract published in *Advance ACS Abstracts,* April 15, 1996.

S0024-9297(95)01843-2 CCC: $12.00

Table 1. Characteristics of SI and hI Samples

code	$10^{-3}M_S$	$10^{-3}M_I$	M_w/M_n
	SI Diblock Copolymer[a]		
SI 14-29	13.9[b]	28.8[c]	1.06
SI 43-86	43.2[b]	85.8[c]	1.06
	hI Matrix[a]		
I-4		4.1	1.05

[a] Cis:trans:vinyl ≅ 75:20:5 for I. [b] Evaluated from M_I and the I/S composition. [c] Determined for precursor I blocks.

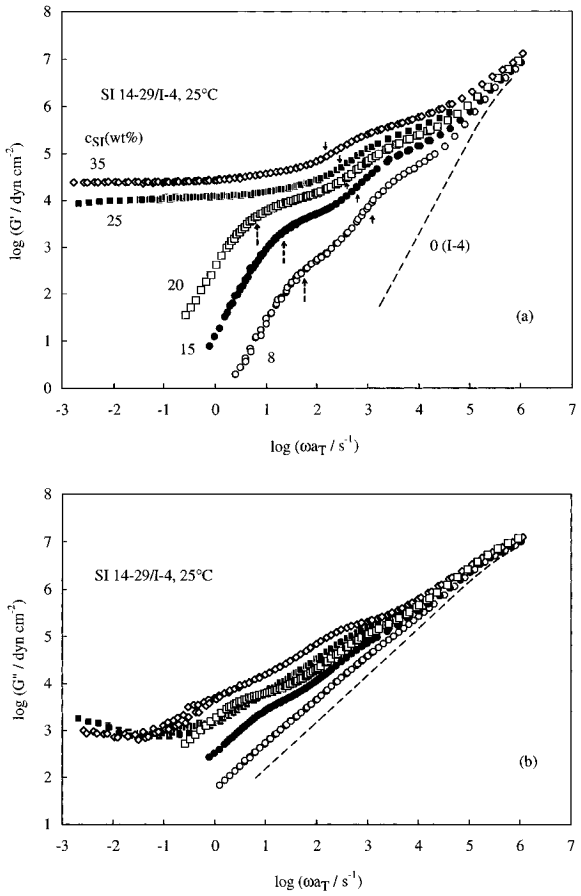

Figure 1. Linear viscoelastic relaxation behavior of SI 14-29/I-4 blends reduced at 25 °C. The dashed curves indicate the behavior of pure matrix I-4. Solid and dashed arrows indicate characteristic frequencies for the fast and slow processes of the micelles, τ^{*-1} and τ_s^{-1}.

nonequilibrium features of the two processes.[18]

II. Experimental Section

II-1. Materials. A linear homopolyisoprene (hI) was anionically polymerized in benzene with *tert*-butyllithium. To ensure a narrow molecular weight distribution (MWD), a seeding technique[19] was used. Two styrene−isoprene (SI) diblock copolymers of narrow MWD were synthesized *via* sequential anionic polymerization in benzene with *sec*-butyllithium: The I blocks were polymerized first, and an aliquot was taken as a precursor. Then, the S blocks were polymerized and terminated with methanol. A fraction of one SI sample, SI 14-29, was terminated with 4-(phenylazo)benzoyl chloride to attach the azobenzene (dye) groups to the S block ends. Diffusion of this dye-tagged sample will be examined in our future paper.

Molecular weights, polydispersity indices, and composition were determined with gel permeation chromatography (GPC) and H-NMR. The results are summarized in Table 1. The I blocks of the SI copolymers as well as the I-4 chains had a large content of 1,4-linkage (≅95% for *cis* plus *trans*) and possessed type-A dipoles parallel along their contour.

II-2. Measurements. SI/I-4 blends with the SI content $c_{SI} \leq 35$ wt % were prepared by first dissolving prescribed amounts of the SI copolymer and the I-4 matrix in benzene to make ≅5% solutions and then allowing benzene to evaporate completely. The S block content in those blends was smaller than 11 vol %. Previous work[4,6,7] on similar SB/hB blends indicates that spherical micelles with S cores were formed in the SI/I-4 blends having such a small S content.

For the SI/I-4 blends and pure I-4 matrix, dielectric losses (ϵ'') were measured with capacitance bridges (GR 1689, GenRad; HP4285A, Hewlett Packard) at temperatures $T = 25-70$ °C. Guarded dielectric cells with vacant capacities of 120 and 130 pF were used. Dynamic mechanical measurements were carried out with a rheometer (RDAII, Rheometrics) at temperatures between −40 and +70 °C. Parallel plates of radius = 1.25 cm were used. For the blends, the viscoelastic responses at low frequencies (corresponding to the slow process of the micelles) became nonlinear even for oscillatory strain of amplitude 0.2. Thus, the strain amplitude was kept below 0.1 (and sometimes below 0.05) to measure dynamic moduli G^* in a linear viscoelastic regime. The ϵ'' and G^* data obeyed the time−temperature superposition and had the same shift factor a_T. Those data were reduced at 25 °C.

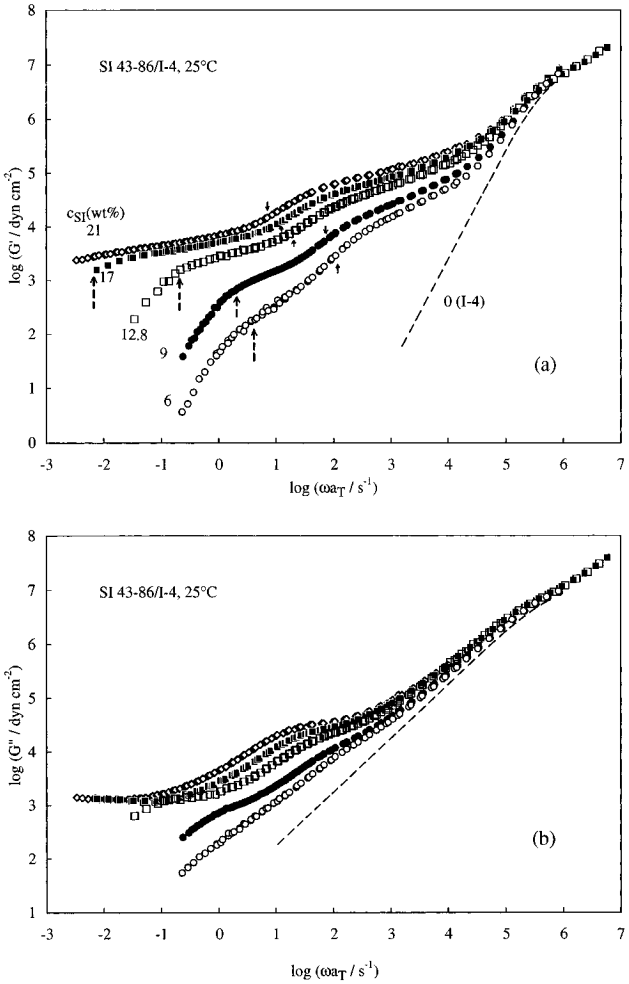

Figure 2. Linear viscoelastic relaxation behavior of SI 43-86/I-4 blends reduced at 25 °C. The dashed curves indicate the behavior of pure matrix I-4. Solid and dashed arrows indicate characteristic frequencies for the fast and slow processes of the micelles, τ^{*-1} and τ_s^{-1}.

III. Results and Discussion

III-1. Overview. Figures 1 and 2, respectively, show frequency (ω) dependence of G^* at 25 °C for the SI 14-29 and 43-86 blends containing spherical micelles with S cores and I corona. The dashed curves indicate G^* of the I-4 matrix. In this short matrix having $M < M_e°$ (=5K; entanglement spacing for bulk PI), the corona I blocks are entangled only when the overlapping micelles

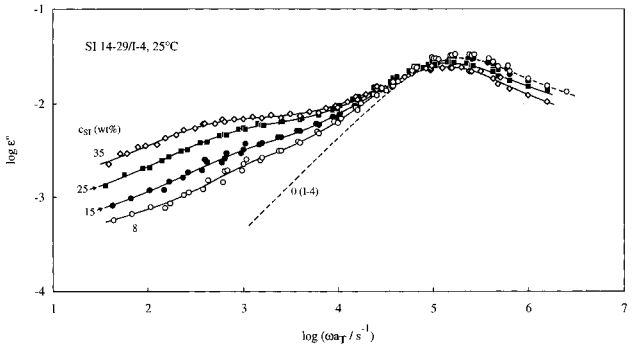

Figure 3. Dielectric relaxation behavior of SI 14-29/I-4 blends reduced at 25 °C. The dashed curves indicate the behavior of pure matrix I-4. The dispersions seen at low $\omega a_T < 10^4$ s^{-1} are attributed to relaxation of the I blocks having type-A dipoles.

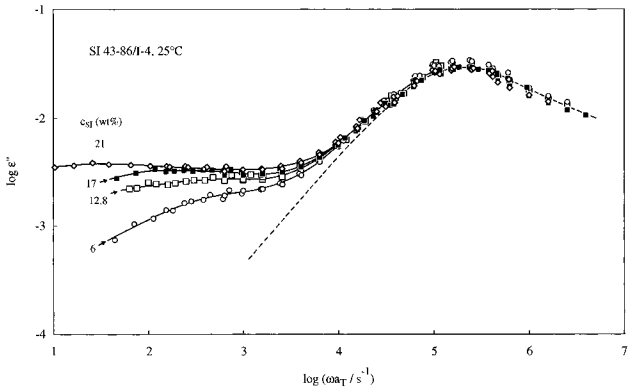

Figure 4. Dielectric relaxation behavior of SI 43-86/I-4 blends reduced at 25 °C. The dashed curves indicate the behavior of pure matrix I-4. The dispersions seen at low $\omega a_T < 10^4$ s^{-1} are attributed to relaxation of the I blocks having type-A dipoles.

satisfy a criterion, $M_{bI}c_{bI}/\rho_I > M_e°$. Here, c_{bI} and M_{bI} are the I block concentration in the matrix phase and the I block molecular weight, respectively, and ρ_I is the bulk I density. As judged from this criterion, the micelles are entangled through their I blocks for $c_{SI} \geq$ 20 wt % (for SI 14-29) and $c_{SI} \geq$ 9 wt % (for SI 43-86).

As seen in Figures 1 and 2, the relaxation of the matrix chains is completed at $\omega a_T \geq 10^5$ s^{-1} (cf. dashed curves). At much longer time scales ($\omega a_T < 10^4$ s^{-1}), we observe two-step relaxation processes that are exclusively attributed to the relaxation of the SB micelles. The thin, solid and thick, dashed arrows, respectively, indicate terminal frequencies of the first and second steps explained later in sections III-2 and III-3. As done in our previous papers,[8] the first relaxation step of the micelles is referred to as the *fast* process, and the second step (corresponding to the terminal relaxation of the blend), as the *slow* process. Note that both fast and slow processes of the micelles are much slower than the matrix relaxation and their relaxation times increase with increasing c_{SI}.

In our experimental window, most of the blends exhibit the terminal relaxation characterized with a relationship, $G' \propto \omega^2$ and $G'' \propto \omega$ at low ω (cf. Figures 1 and 2). As explained in the Introduction, the osmotic requirement for the corona I blocks should have been effectively screened by the matrix I-4 chains in those blends and thus the SI micelles should have been randomly dispersed to exhibit the terminal viscoelastic relaxation. The exception is for the SI 14-29 blends with $c_{SI} = 25$ and 35 wt % (Figure 1) that exhibit an unrelaxed plateau in G' and a very small loss ($G'' \ll G'$) at low ω. For these blends containing fairly concentrated I blocks ($c_{bI} = 0.17$ and 0.25 g cm^{-3}, respectively), the matrix I-4 chains appear to be incapable of completely screening the osmotic requirement, thereby allowing the SI micelles to form macrolattices and exhibit plasticity. The plateau in G' reflects elastic behavior of the macrolattice before yielding.[1] Even for those blends containing the macrolattice, the fast process of the micelles is clearly observed at $\omega a_T = 10^2-10^4$ s^{-1}.

The other feature to be noted in Figures 1 and 2 is the shape (ω dependence) of the G' and G'' curves that reflects the relative distribution of linear viscoelastic relaxation modes. In the terminal region of the fast process (specified with the thin, solid arrows), the shape of those curves does not change much with c_{SI} (in particular for G') and thus the mode distribution is insensitive to c_{SI}. As explained later, this c_{SI} insensitivity of the mode distribution for the fast process is utilized for evaluation of the relaxation times for this process.

Figures 3 and 4, respectively, show ϵ'' data for the SI 14-29 and 43-86 blends at 25 °C. The dashed curves indicate the behavior of the I-4 matrix. Global motion of the I blocks and I-4 matrix chains having type-A dipoles leads to dielectric relaxation.[10−13,20−22] In Figures 3 and 4, the matrix relaxation is observed as the ϵ'' peak at $\omega a_T \cong 2 \times 10^5$ s^{-1}. At much longer time scales ($\omega a_T < 10^4$ s^{-1}), dielectric relaxation of the I blocks is observed as shoulders in the ϵ'' curves. At those long time scales where the matrix has relaxed, the dielectric relaxation function $\Phi(t)$ of the blend is related to end-to-end vector $\mathbf{R}_p$ of the pth I block,[10,20−23]

$$\Phi(t) \propto \sum_p \sum_q \langle \mathbf{R}_p(t)\cdot\mathbf{R}_q(0)\rangle = \sum_p \langle \mathbf{R}_p(t)\cdot\mathbf{R}_p(0)\rangle + \sum_{p\neq q} \langle \mathbf{R}_p(t)\cdot\mathbf{R}_q(0)\rangle \quad (1)$$

Here, the first term represents an auto-correlation for respective I blocks and the second term indicates a cross-correlation for different I blocks. For randomly orientated and incoherently moving linear homopolyisoprene chains, the second term vanishes.[20,23] However, this is not necessarily the case for the micelles examined here, as discussed later in section III-3.

In Figures 3 and 4, the dielectric relaxation of the I blocks is observed at frequencies similar to those for the fast viscoelastic process of the micelles (Figures 1 and 2). It should also be noted that the terminal dielectric relaxation characterized with a relationship, $\epsilon'' \propto \omega$, is *not* attained for the blends even at low ω where the fast viscoelastic process is completed: For example, for the 8 wt % SI 14-29/I-4 blend the fast process is completed at $\omega a_T \cong 10^3$ s^{-1} (Figure 1) but the ϵ'' curve exhibits only a weakly ω-dependent tail down to $\omega a_T \cong 50$ s^{-1} (Figure 3). These results indicate that both fast and slow viscoelastic processes of the micelles (Figures 1 and 2) are dielectrically active. In other words, both processes should be governed by mechanisms that induce changes in either the auto-correlation or cross-correlation of the end-to-end vectors of the I blocks (eq 1).

As explained in part 2, nonlinearity in stress relaxation behavior of the SI micelles is much less significant for the fast process than for the slow process.[18] This fact demonstrates differences in the relaxation mechanisms for these processes. The fast process exhibits nonlinearity similar to that for homopolymers[18] and quite possibly reflects the relaxation of individual corona I blocks, being in harmony with our previous assign-

ment.[8] On the other hand, the slow process would be attributed to collective motion of the I blocks. Previous studies related this motion to diffusion of micelles.[6−8] In the remaining part of this paper, we further test these molecular assignments, considering the fact that both fast and slow processes are dielectrically active.

III-2. Features of the Fast Process. The viscoelastic relaxation behavior of individual I blocks tethered on the rigid S cores should be similar to that of star-branched homopolyisoprene (hI) chains. For both relaxation mode distribution and relaxation time τ, the star chains exhibit characteristic features: For solutions of star chains with arm molecular weight M_a and concentration c,[24] the mode distribution is universally scaled by a factor c/M_a and τ in the entangled regime increases exponentially with $M_a/M_e(c)$, where $M_e(c)$ is the entanglement spacing in the solutions. These features are in contrast to those of entangled solutions of linear chains[25] for which the mode distribution is scaled by a different factor, $c/M_e(c)$, and τ is proportional to $M^{3.5}/M_e(c)^{1.5}$.

If the fast viscoelastic process of the SI micelles corresponds to the relaxation of individual I blocks, similarities between this process and star relaxation should be found not only for the relaxation time but also for the relaxation mode distribution. These similarities are examined in the remaining part of this section, first for the mode distribution and then for the relaxation time.

Relaxation Mode Distribution. The universal viscoelastic mode distribution of star chains explained above is most clearly observed as universal superposition of reduced moduli, $G_r^* = [M_a/cRT]G^*$, plotted against reduced frequencies, $\omega\tau$.[8,24] (Note that the mode distribution is sensitively reflected in the shape (ω dependence) of the G^* curves.) Thus, we examine whether the fast process of the SI micelles exhibits similar universality for $G_r^* = [M_{bI}/c_{bI}RT]G^*_{SI}$, with G^*_{SI} being the contribution of the micelles to G^*_{blend}.

As done for homopolymer blends,[25,26] G^*_{SI} was evaluated from G^*_{blend} data,

$$G^*_{SI}(\omega) = G^*_{blend}(\omega) - \phi_{I\text{-}4}G^*_{I\text{-}4}(\omega) \qquad (2)$$

Here, $\phi_{I\text{-}4}$ and $G^*_{I\text{-}4}$ are the volume fraction and dynamic moduli of the matrix chains in the blends. Since the I blocks are not very concentrated in the matrix phases ($c_{bI} \leq 0.25$ g cm^{-3}), the behavior of the matrix would be hardly affected by the I blocks. Thus, $G^*_{I\text{-}4}$ of the pure matrix was used in eq 2 to evaluate G^*_{SI}. It should be emphasized that G'_{blend} is much larger than $G'_{I\text{-}4}$ at time scales of the fast and slow processes of the micelles (cf. Figures 1a and 2a) and the subtraction of $G^*_{I\text{-}4}$ (eq 2) is a very minor correction for G'_{SI} at those time scales.

Figures 5 and 6 compare the G_r^* curves for the SI 14-29 and 43-86 micelles. The solid curves indicate G_r^* for bulk, 4-arm star-hI of $M_a = 36.7$K (Figure 5) and $M_a = 95$K (Figure 6) reported by Fetters et al.[27] These M_a values are close to M_{bI} of the I blocks, in particular for the case of the SI 43-86 micelles. For respective star-hI chains, the terminal relaxation time τ_{star} was evaluated as the product of the viscosity and compliance and G_r^* were plotted against the reduced frequency, $\omega\tau_{star}$.

In Figures 5 and 6, the G_r^* curves for the SI micelles are shifted along the ω axis by factors τ^* so that they are best superposed on the curves for the star-hI. Around the low-ω end of the fast process ($\omega\tau^* \cong 1-20$), the G_r' curves of the micelles are well superposed with each other and also with the G_r' curves of the star-hI. Since the contribution of very rapid relaxation (at $\omega\tau^*$

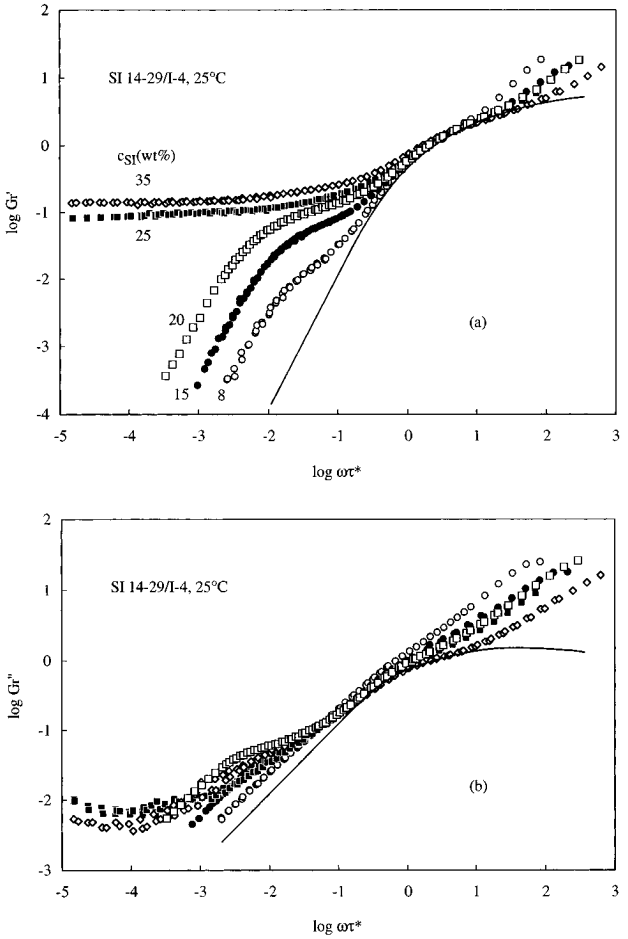

Figure 5. Plots of reduced moduli $G_r^* = [M_{bI}/c_{bI}RT]G^*_{SI}$ against $\omega\tau^*$ for the SI 14-29 blends. The solid curves indicate reduced moduli for a 4-arm star hI ($M_a = 36.7$ K)[27] plotted against $\omega\tau_{star}$.

≥ 100) is much larger for G_r'' than for G_r', poorer superposition is observed for G_r''. However, subtraction of this contribution improved the superposition for G_r''.

The above results indicate that the viscoelastic mode distribution of the fast process of the micelles is almost universally scaled by M_{bI}/c_{bI} and close to the distribution for star-hI chains, supporting the assignment of this process to starlike relaxation of individual corona blocks. Similar results were found previously also for SB micelles.[8] The other important feature to be noted in Figures 5 and 6 is the good superposition of the G_r^* curves for the SI micelles on the star-hI curves, the latter being plotted against frequencies scaled by the measured relaxation time τ_{star}. This result indicates that τ^* gives the viscoelastic relaxation time for the fast process of the micelles.[8] In fact, the characteristic frequency τ^{*-1} indicated in Figures 1 and 2 (thin, solid arrows) well specifies the low-ω ends of the fast process. (In general, the superposition of G^* curves, if it works, enables us to most accurately evaluate the characteristic time of a relaxation process followed by slower processes.) The c_{bI} and M_{bI} dependence of τ^* is later examined in Figures 9−11.

As done for the viscoelastic moduli, the contribution of the SI micelles to the dielectric loss of the blend is evaluated as

$$\epsilon''_{SI}(\omega) = \epsilon''_{blend}(\omega) - \phi_{I\text{-}4}\epsilon''_{I\text{-}4}(\omega) \qquad (3)$$

Here, $\epsilon''_{I\text{-}4}$ is the dielectric loss for the pure matrix I-4 (dashed curves in Figures 3 and 4). We examine whether the ϵ''_{SI} curves exhibit universal superposition

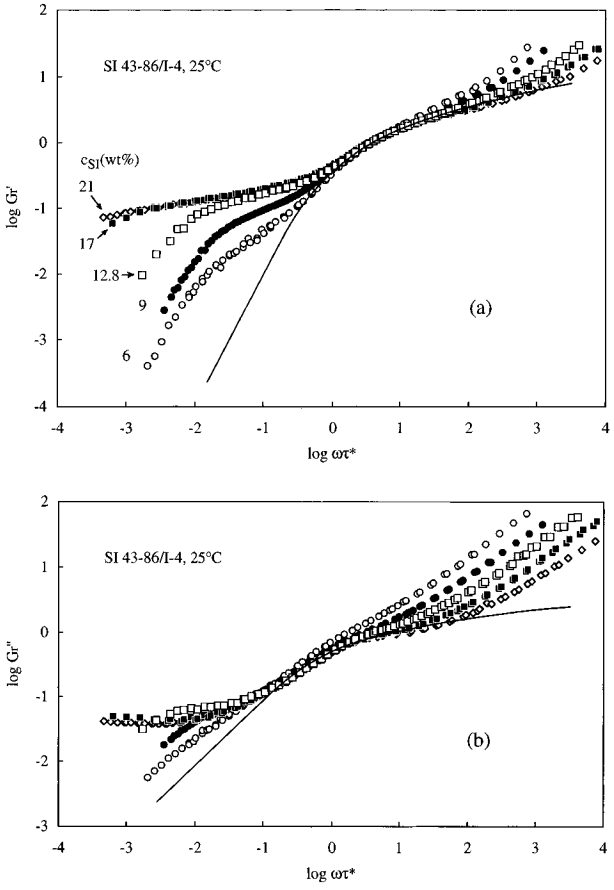

Figure 6. Plots of reduced moduli $G_r^* = [M_{bI}/c_{bI}RT]G^*_{SI}$ against $\omega\tau^*$ for the SI 43-86 blends. The solid curves indicate reduced moduli for a 4-arm star hI (M_a = 95K)[27] plotted against $\omega\tau_{star}$.

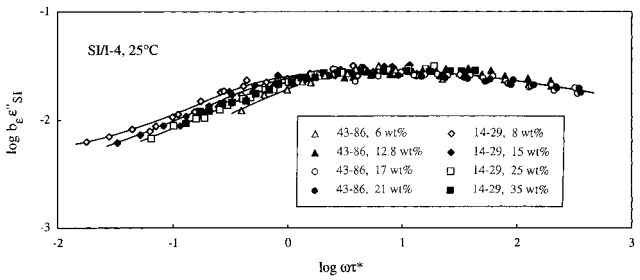

Figure 7. Plots of reduced dielectric loss $b_\epsilon\epsilon''_{SI}$ against $\omega\tau^*$ for the SI 14-29 and 43-86 micelles.

similar to that for G_r^* (Figures 5 and 6). For this purpose, we compared the dependence of reduced dielectric losses of the micelles, $b_\epsilon\epsilon''_{SI}$, on the reduced frequency defined for G_r^*, $\omega\tau^*$. Here, b_ϵ^{-1} is a reduction factor for the dielectric intensity. Figure 7 shows the comparison at low ω where the subtraction of the matrix contribution (eq 3) brought little uncertainties in ϵ''_{SI}. The dependence of the b_ϵ^{-1} factors on the volume fraction ϕ_{bI} of the I blocks in the blends is shown in Figure 8.

As noted in Figure 7, good superposition is achieved for the $b_\epsilon\epsilon''_{SI}$ curves of the SI 14-29 and 43-86 micelles at $\omega\tau^* \geq 1$. This result indicates that the fast viscoelastic process of the SI micelles is accompanied by dielectric relaxation of nearly universal mode distribution (observed as nearly identical shapes of the $b_\epsilon\epsilon''_{SI}$ curves at $\omega\tau^* \geq 1$) and the dielectric relaxation time is in a vicinity of the viscoelastic τ^*. The good superposition of the $b_\epsilon\epsilon''_{SI}$ curves also indicates that the dielectric relaxation intensity $\Delta\epsilon_f$ accompanying the fast viscoelastic process is proportional to b_ϵ^{-1}. Thus, as noted

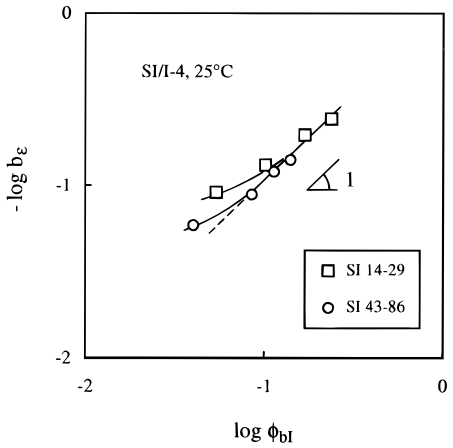

Figure 8. Dependence of the dielectric intensity reduction factors b_ϵ^{-1} for the fast process on the I block volume fraction ϕ_{bI} in the matrix phase.

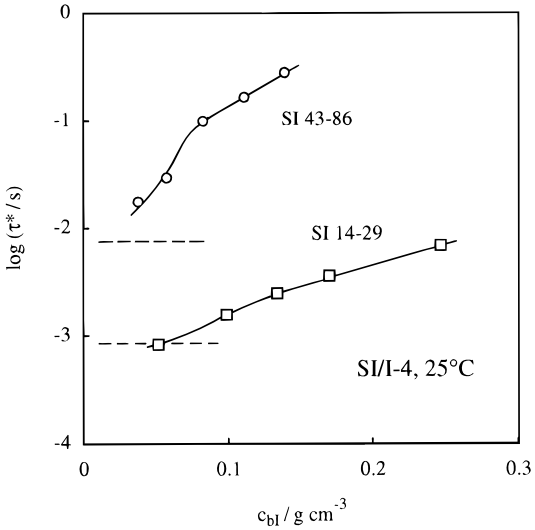

Figure 9. Dependence of the relaxation time τ^* for the fast process of SI 14-29 and 43-86 micelles at 25 °C on the I block concentration c_{bI} in the matrix phase. The horizontal dashed lines indicate Rouse relaxation times τ_{Rouse} for the tethered I blocks evaluated from data[21,22] for low-M hI chains. The τ^* data and τ_{Rouse} are compared at an isofrictional state.

in Figure 8, $\Delta\epsilon_f$ is proportional to ϕ_{bI} for large ϕ_{bI} but upward deviation emerges for small ϕ_{bI}. These dielectric features are similar to those of hI chains:[20,22] coincidence of dielectric and viscoelastic relaxation times (within a factor of 2), proportionality between $\Delta\epsilon$ and ϕ for concentrated solutions, and upward deviation of $\Delta\epsilon$ in dilute solutions in good solvents. These similarities again suggest that the fast viscoelastic process reflects the relaxation of individual corona I blocks, although effects of the S cores on the I block motion as well as a solvent quality of the I-4 matrix for the I blocks need to be incorporated in more detailed consideration for the dielectric features. The similarities also suggest that the dielectric relaxation accompanying the fast viscoelastic process of the micelles corresponds to the autocorrelation for the I blocks (the first term in eq 1).

Relaxation Time. Figure 9 shows semilogarithmic plots of the relaxation time τ^* of the fast viscoelastic process of the SI micelles against the I block concentration c_{bI} in the matrix phase. As mentioned earlier, c_{bI} is not very large ($c_{bI} \leq 0.25$ g cm^{-3}) for the micelles examined here so that the segmental friction ζ_{bI} for the I blocks is essentially determined by the matrix I-4 chains. Since ζ for this short matrix (M = 4.1K) is smaller than ζ for high-M hI chains, we analyzed a_T for

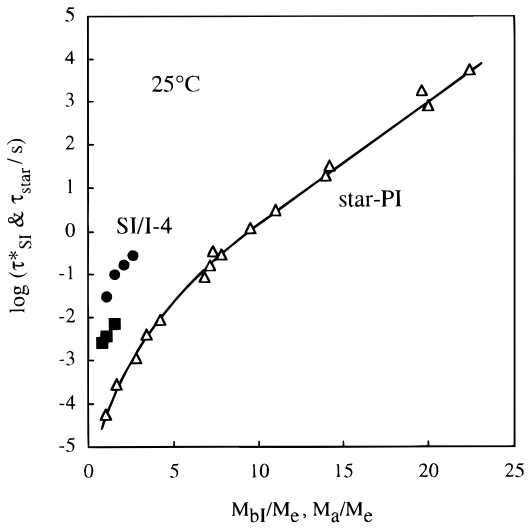

Figure 10. Dependence of the relaxation time τ^*_{SI} for the fast processes of entangled SI 14-29 (filled squares) and SI 43-86 micelles (filled circles) at 25 °C on the M_{bI}/M_e ratio. The unfilled triangles indicate τ_{star} data (25 °C) for entangled, 4-, 5-, 8, and 12-arm star hI chains[27,28] being plotted against M_a/M_e. The τ^* data are compared with the τ_{star} data at an isofrictional state.

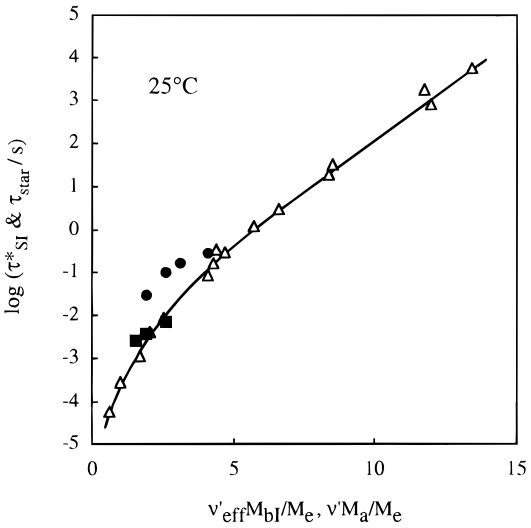

Figure 11. Plots of τ^*_{SI} for the fast process of SI micelles and τ_{star} for entangled star hI chains against $\nu'_{eff}M_{bI}/M_e$ and $\nu'M_a/M_e$, respectively. The symbols are the same as in Figure 10.

both viscoelastic and dielectric data for the I-4 matrix to carry out ζ corrections for the τ^* data of the micelles. The correction factor, $\zeta/\zeta_\infty = 0.5$ with ζ_∞ being ζ for high-M hI, agreed with previous results for low-M hI chains.[21,22] In Figures 9−11, the τ^* data after this correction are shown. Those data can be directly compared with τ_{star} of high-M, bulk hI chains at 25 °C.

From viscoelastic and dielectric data for low-M hI chains,[21,22] the Rouse relaxation times τ_{Rouse} were evaluated for tethered I blocks at the iso-ζ state (25 °C). In Figure 9, τ_{Rouse} are indicated with the horizontal dashed lines. As seen there, τ^* for the SI micelles is close to τ_{Rouse} for small c_{bI} but increases exponentially with c_{bI} for large c_{bI}. This exponential increase is characteristic to entangled star chains,[27,28] supporting the molecular assignment of the fast process of the micelles to the starlike relaxation of individual I blocks.

The terminal relaxation time τ_{star} of entangled star chains is essentially scaled as $\exp[\nu' M_a/M_e]$,[27,28] where ν' is a constant ($\cong$0.6 for hI[27,28]) and M_e is the entangled spacing ($M_e \cong M_e^\circ \rho_I/c_I$ for blends in short matrices). Thus, if the features of the relaxation of individual I blocks (fast viscoelastic process of the micelles) are exactly the same as those for the star-hI chains, the τ^*_{SI} *vs* M_{bI}/M_e plots for the micelles should coincide with the τ_{star} *vs* M_a/M_e plots for star-hI. Figure 10 examines this expectation for the entangled I blocks having $M_{bI} \geq M_e$. As seen there, τ^*_{SI} (filled symbols) is 2−3 orders of magnitudes larger than τ_{star} for entangled star-hI (triangles).[27,28] This result demonstrates differences in the relaxation behavior of the I blocks and star-hI. In our previous work,[8] similar differences were related to effects of S cores in the following way.

For relaxation of entangled star chains, the tube model[28−30] considers retraction of the star arm that is retarded by an activation barrier of entropic nature. For the arm having no impenetrable domain, distribution of its contour length L measured along the tube is Gaussian and the corresponding activation barrier for the arm retraction is given by a quadratic function of L,[28−30]

$$\Delta U^o(L) = \nu'(M_a/M_e)kT[1 - (L/L_{eq}^o)]^2 \qquad (4)$$

Here, L_{eq}^o is the equilibrium L value and ν' is a constant ($\cong$0.6 for star-hI). The relaxation time for the arm is essentially scaled as $\exp[\Delta U^o(\xi)/kT]$, with ξ ($\propto M_e^{1/2}$) being a small, critical contour length to which the arm has to retract to escape from the tube. Well-entangled star arms have $L_{eq}^o \gg \xi$ and $\Delta U^o(\xi) \cong \nu' kTM_a/M_e$, leading to the exponential M_a/M_e dependence of τ_{star}.[28−30]

The entangled I blocks are considered to relax *via* a similar retraction mechanism. However, differing from the star arms, the I blocks are tethered on impenetrable S cores and their retraction should be disturbed by the cores. In particular, if the S core is comparable in size with the I block, the core would behave as a flat, impenetrable wall when the I block end retracts to a vicinity of the core. For this case, the contour length L of the I block should have a non-Gaussian distribution[8,31] and the corresponding activation barrier for the retraction can be evaluated as[8]

$$\Delta U(L) = 2\nu'(M_{bI}/M_e)kT[1 - (L/L_{eq})]^2 + kT[(L/L_{eq}) - 1 - \ln(L/L_{eq})] \quad \text{for small } L \qquad (5)$$

The relaxation time τ^* for the I block is scaled as $\exp[\Delta U(\xi)/kT]$, with ξ being the escape length.

Equations 4 and 5 indicate that $\Delta U(\xi)$ is considerably larger than $\Delta U^o(\xi)$ and thus τ^* is much longer than τ_{star}, being in harmony with the results seen in Figure 10. For further comparison of τ^* and τ_{star}, we attempted to approximate $\Delta U(L)$ in a range of $L \geq \xi$ by a quadratic function of L/L_{eq},[8]

$$\Delta U(L) \cong (\nu'_{eff}/\nu')\Delta U^o(L) = \nu'_{eff}(M_{bI}/M_e)kT[1 - (L/L_{eq})]^2 \quad \text{for } L_{eq} \geq L \geq \xi \qquad (6)$$

Here, ΔU^o is an activation barrier for the corresponding star arm and ν'_{eff} is a numerical factor larger than ν'. As similar to previous results for SB micelles,[8] $\Delta U(L)$ for the I blocks (eq 5) were well fitted with this approximate expression in a range $L_{eq} \geq L \geq \xi$, and the ν'_{eff} values were evaluated from this fit. Since τ^* and τ_{star} are essentially proportional to $\exp[\Delta U^o(\xi)/kT]$ and $\exp[\Delta U(\xi)/kT] \cong \exp[\nu'_{eff}\Delta U^o(\xi)/\nu' kT]$, we expect coincidence of τ^* and τ_{star} being plotted against $\nu'_{eff}M_{bI}/M_e$ and $\nu' M_a/M_e$, respectively (cf. eqs 4−6). This expectation is examined in Figure 11.

As noted in Figure 11, the orders-of-magnitude differences of τ_{star} and τ^* seen in Figure 10 are largely reduced in the plots against $\nu'_{eff}M_{bI}/M_e$ and $\nu'M_a/M_e$. Similar reduction was found also for SB micelles.[8] These results are in harmony with the above expectation, indicating that the entangled I blocks of the SI micelles relax quite possibly *via* the starlike retraction that is retarded by the impenetrable S cores. This relaxation process is observed in Figures 1 and 2 as the fast viscoelastic processes of the micelles.

However, in Figure 11, nontrivial differences still remain between τ_{star} and τ^*_{SI}. Equation 5 neglects spatial confinement for the I blocks due to S cores of *neighboring* micelles, and those differences may be related to this confinement: Some portion of the I block would take hairpin-like conformation to ooze from the tube during the retraction process. The neighboring S cores may disturb this oozing process to induce additional retardation for the I block retraction. It is desired to formulate a tube model considering the confinements from all S cores and compare the calculated dynamic quantities of the I blocks with those of entangled star chains. This is considered as future work.

III-3. Features of the Slow Process. As noted in Figures 5 and 6, the universality of the G^*_{SI} curves scaled by the factor $[M_{bI}/c_{bI}RT]$ is valid for the fast process of the micelles but not for the slow process. In addition, nonlinear stresss relaxation behavior is quite different for these processes.[18] These results indicate differences in the relaxation mechanisms of the two processes.

Here, we examine whether a different type of universality exists for G_r^* for the slow process. For this purpose, we evaluated relaxation time τ_s of this process in the following way. When the SI/I-4 blends exhibit the terminal behavior characterized with the relationships $G' \propto \omega^2$ and $G'' \propto \omega$, τ_s is evaluated from G^*_{SI} of the micelles (eq 2) as

$$\tau_s = [(G'_{SI}/\omega^2)(G''_{SI}/\omega)^{-1}]_{\omega\to 0} \qquad (7)$$

This τ_s gives an average relaxation time (often referred to as a *weight-average* relaxation time) that is close to the longest relaxation time of the micelles. For the SI 14-29 blends with $c_{SI} \le 20$ wt % and the SI 43-86 blends with $c_{SI} \le 12.8$ wt %, the terminal behavior is observed in our experimental window (Figures 1 and 2) and τ_s was determined from eq 7. Characteristic frequencies τ_s^{-1} shown in Figures 1 and 2 (thick, dashed arrows) well specify the low-ω ends of the slow process.

At low ω, the fast viscoelastic process hardly contributes to G'_{SI} so that the mode distribution for the slow process can be examined from comparison of the G'_{SI} curves. Thus, using $\omega\tau_s$ as the reduced frequency, we examined whether superposition is achieved for the G'_{SI}-($\omega\tau_s$) curves with intensities being scaled by appropriate factors, b_s/RT. The results are shown in Figure 12 where the G'_{SI} curve for the 20 wt % SI 14-29 blend is used as a reference for the superposition ($b_s = 1$). For the 17 wt % SI 43-86 blend exhibiting only the onset of the terminal relaxation, an adequately shifted G'_{SI} curve is also shown (filled diamonds). Including this blend, fairly good superposition is seen for the $b_sG'_{SI}/RT$ curves at low $\omega\tau_s$. This result means that the micelles have roughly the same terminal mode distribution for the slow process and their terminal relaxation intensities are proportional to b_s^{-1}.

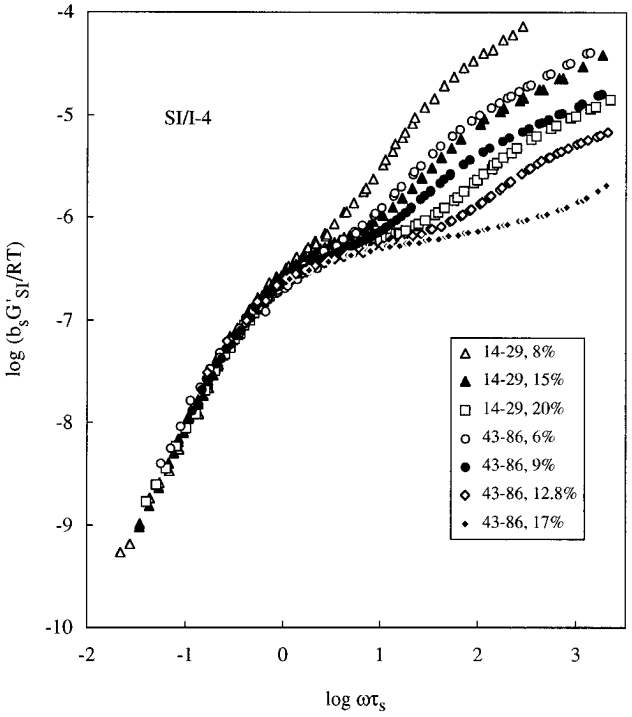

Figure 12. Reduced storage moduli $b_sG'_{SI}/RT$ at 25 °C for the SI 14-29 and 43-86 micelles of various c_{SI} as indicated. The moduli are plotted against reduced frequencies $\omega\tau_s$, with τ_s being the relaxation time for the slow process of the micelles.

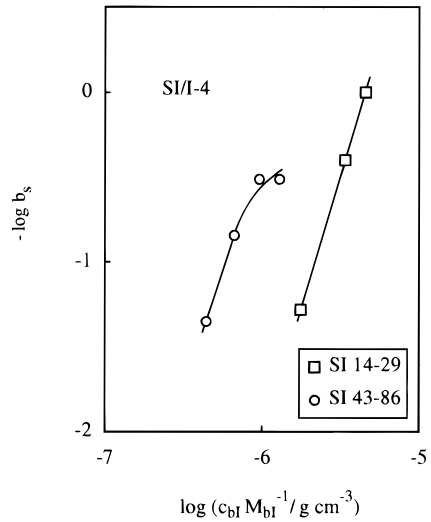

Figure 13. Dependence of the viscoelastic intensity factor b_s^{-1} for the slow process on c_{bI}/M_{bI}^{-1}.

Figure 13 shows the dependence of the intensity factor b_s^{-1} on $c_{bI}M_{bI}^{-1}$. Clearly, b_s^{-1} is not uniquely determined by $c_{bI}M_{bI}^{-1}$. This result is in contrast to that for the fast process for which G^*_{SI} is scaled by M_{bI}/c_{bI} and thus the terminal intensity is proportional to $c_{bI}M_{bI}^{-1}$ (Figures 5 and 6). This fact again demonstrates differences between the slow and fast processes of the micelles. We also note in Figure 13 that for each series of the blends, b_s^{-1} exhibits strong c_{bI} dependence for small c_{bI} but the dependence becomes weaker for large c_{bI}.

In previous studies,[6−8] the slow process of the micelles was attributed to diffusion of the micelles: Anisotropy in spatial distribution of the micelles due to applied strain generates mechanical stress, and diffusion of the micelles is required for relaxation of this stress. If the slow process is governed by the simplest Stokes−Einstein (SE) mechanism, τ_s should agree with the SE

diffusion time,

$$\tau_{SE} = \pi R_m \eta_{eff} \delta^2 / kT \quad (8)$$

Here, δ is a diffusion distance required for the recovery of isotropic distribution of the micelles, R_m is the micelle radius, and η_{eff} is an effective viscosity for the micelle diffusion. R_m is estimated as $0.5d_S + 2^{1/2}R_{I,\theta}$, with d_S and $R_{I,\theta}$ being the *S* core diameter and the unperturbed end-to-end distance of the I blocks.[8] (The factor $2^{1/2}$ for $R_{I,\theta}$ accounts for expansion of the I block dimension due to the effects of impenetrable S cores.[8]) d_S were estimated from SAXS data for structurally similar SB micelles,[2] and $R_{I,\theta}$ were evaluated from data for hI chains[32] ($d_S \cong 160$ and 310 Å and $R_{I,\theta} \cong 140$ and 240 Å for the SI 14-29 and 43-86 micelles, respectively). For simplicity, δ was taken to be the micelle diameter, $2R_m$.

As discussed previously,[8] η_{eff} can be related to the fast viscoelastic process of the micelles in the following way. For concentrated micelles entangled through their corona I blocks, the micelle diffusion would be disturbed until the I block relaxation is completed. For this case, the relaxation of individual I blocks would determine the diffusion rate and thus η_{eff} would be close to a viscosity η_{fast} associated with the I block relaxation. For the SI micelles, this relaxation is observed as the fast process (Figures 1 and 2) and the G_r* curves for this process are close to the curves for the star-hI chains (Figures 5 and 6). This enabled us to evaluate η_{fast} ($\cong\eta_{eff}$) from the known viscosity of the star-hI.

The situation changes for dilute and nonentangled micelles. The relaxation of individual I blocks would not be necessarily required for diffusion of such dilute micelles: For example, even if the I blocks do not relax but behave as a purely elastic corona, the dilute micelles can still exhibit diffusion. Thus, for the dilute micelles, η_{eff} may be smaller than η_{fast} and the diffusion time may be shorter than τ_{SE} evaluated from η_{fast}. In an extreme case, η_{eff} is given by the viscosity η_{mat} of the matrix and the SE diffusion time becomes

$$\tau_{SE}^{o} = \pi R_m \eta_{mat} \delta^2 / kT \quad (9)$$

If the slow process of the micelles is governed by the simplest SE mechanism, τ_s can *never* be shorter than τ_{SE}^{o}. In other words, τ_{SE}^{o} gives the lowest bound for τ_s of the slow process attributable to the SE diffusion.

Figure 14 compares τ_s and τ_{SE} for the SI micelles (large filled symbols). For both entangled and nonentangled micelles, τ_{SE} were evaluated from eq 8 with η_{eff} being replaced by η_{fast}. The numbers attached to the large symbols indicate c_{SI} (in wt %) of the micelles. As explained for Figure 12, the 17 wt % SI 43-86 micelle exhibits only the onset of the terminal relaxation and its τ_s was not evaluated by eq 7. For this blend, τ_s was determined from the superposition of the G_{SI}' curve (Figure 12). For the other SI micelles, τ_s was determined by eq 7.

In Figure 14, the thin solid line represents a relationship, $\tau_s = \tau_{SE}$. The small circles indicate previous data for SB micelles[8] of various molecular weights and concentrations in a short, nonentangling hB matrix, and the small triangles indicate those in long, entangling hB matrices. For both dilute and concentrated SB micelles, the τ_s data are plotted against τ_{SE} evaluated for $\eta_{eff} = \eta_{fast}$ (eq 8). For those micelles, previous studies[8] indicated that the relationship between τ_s and τ_{SE} changes with the extent of entanglements between the corona blocks in the following way (cf. Figure 10 in ref 8a and Figure 6 in ref 8b): When the micelles are

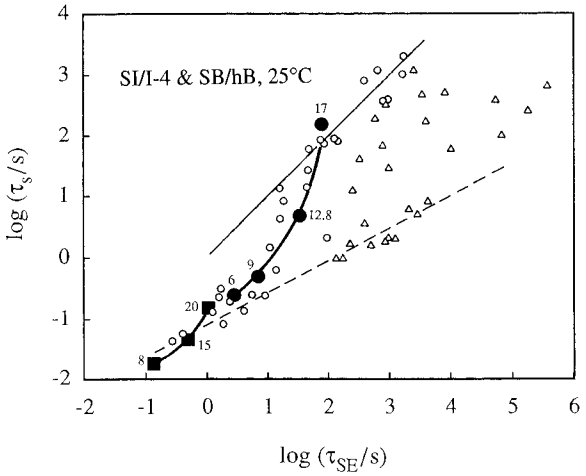

Figure 14. Plots of the relaxation times τ_s for the slow process of SI 14-29 (large filled squares) and SI 43-86 (large filled circles) micelles against the Stokes−Einstein (SE) diffusion time τ_{SE} evaluated for $\eta_{eff} = \eta_{fast}$. The numbers attached to those symbols indicate c_{SI} (in wt %). Small circles and triangles indicate τ_s data (25 °C)[8] obtained for SB micelles in a nonentangling hB matrix (M = 2K) and entangling hB matrices ($M \geq$ 27.6K), respectively. The thin solid line indicates the relationship, $\tau_s = \tau_{SE}$.

dilute and nonentangled through their corona blocks, τ_s is considerably smaller than τ_{SE}. Those τ_s data exhibit a rather weak dependence on τ_{SE} and are collapsed around the dashed line in Figure 14. This dependence becomes stronger with increasing micelle concentration. Finally, for concentrated micelles well entangled through their corona blocks, τ_s are close to τ_{SE} irrespective of the corona concentration and molecular weight.

As noted in Figure 14, the behavior of the SI micelles (large filled symbols) is similar to that of the SB micelles: The τ_s data for the nonentangled SI micelles (c_{SI} = 8 and 15 wt % for SI 14-29 and 6 wt % for SI 43-86) are located in the vicinity of the dashed line. The data exhibit upward deviation from this line as the entanglement between the micelles is developed (c_{SI} = 20 wt % for SI 14-29 and 9 and 12.8 wt % for SI 43-86). Finally, for moderately entangled SI 43-86 micelles (c_{SI} = 17 wt %), τ_s is located near the thin solid line representing the relationship $\tau_s = \tau_{SE}$.

The above results for the SI and SB micelles strongly suggest that the slow relaxation processes of the *concentrated* micelles are attributed to their SE diffusion with the effective viscosity being determined by the corona block relaxation. On the other hand, for the dilute micelles, τ_s is significantly shorter than τ_{SE}. For such dilute micelles, one may expect that the slow process is still governed by the SE mechanism but η_{eff} is close to η_{mat} of the pure matrix, not to η_{fast}. To test this expectation, we examine a relationship between τ_s and τ_{SE}^{o} (eq 9) in Figure 15. The large symbols indicate τ_s data for the dilute SI micelles in the nonentangling I-4 matrix. The small circles and triangles denote the data for *dilute* SB micelles[8] in short (nonentangling) and long (entangling) hB matrices, respectively. The solid line represents the relationship, $\tau_s = \tau_{SE}^{o}$.

In Figure 15, we note that τ_s of the dilute SI and SB micelles in the *nonentangling* matrices are collapsed in the vicinity of the solid line. Thus, the slow process of those dilute micelles appears to reflect the SE diffusion in the pure matrix. However, we also note that τ_s for the dilute SB micelles in the *entangling* matrices (triangles) are much shorter than τ_{SE}^{o} and the simplest SE diffusion cannot be the mechanism for the slow process of those micelles. (Remember that τ_{SE}^{o} gives

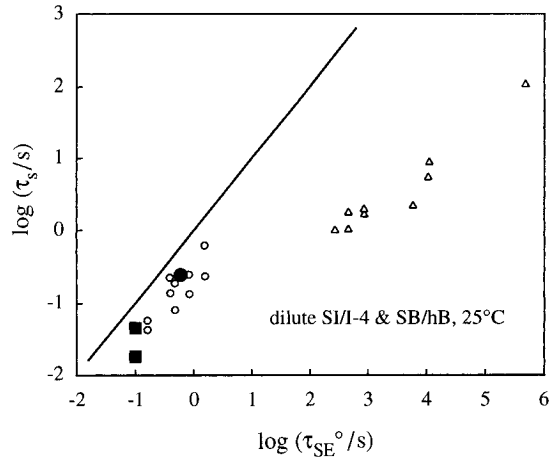

Figure 15. Plots of τ_s for the slow process of dilute SI 14-29 and SI 43-86 micelles against the SE diffusion time τ_{SE}^{o} evaluated for $\eta_{eff} = \eta_{mat}$ (large filled symbols). Small circles and triangles indicate τ_s for dilute SB micelles[8] in a nonentangling hB matrix (M = 2K) and entangling hB matrices ($M \geq$ 27.6K), respectively. The solid line indicates the relationship, $\tau_s = \tau_{SE}^{o}$.

the lowest bound for the SE diffusion time.) Thus, the slow relaxation mechanism of the dilute micelles might change with the extent of the matrix entanglement. Further studies are necessary for this problem. Specifically, it is desired to compare τ_s with experimentally determined micelle diffusion times. An attempt is now being made, and the results will be presented in our forthcoming paper.

Finally, we would like to add a few comments on features of the slow viscoelastic process of the micelles. This process is dielectrically active (cf. Figures 3 and 4), meaning that the orientational memory of the I blocks survives to some extent up to the time scales of this process (cf. eq 1). Since the I blocks are tethered on the impenetrable S cores, motion of the S cores would be required for complete decay of the memory for individual I blocks. This argument suggests that the auto-correlation term shown in eq 1 contributes to the dielectric relaxation accompanying the slow process. In addition, for different I blocks tethered on the same S core, the cross-correlation (the second term in eq 1) may also contribute if the I blocks are coherently dragged by the S core. (This type of cross-correlation may become significant when many I chains are bound together at their ends.) These considerations suggest that the slow process is related to the motion of the S cores, being in harmony with the above assignment for the entangled micelles.

IV. Concluding Remarks

We have examined features of the fast and slow relaxation processes of the SI micelles that are detected both viscoelastically and dielectrically. The fast process exhibits features similar to the relaxation of star chains: nearly universal mode distribution of G_r* scaled by the factor $M_{bI}/c_{bI}RT$ (Figures 5 and 6), nearly universal mode distribution of ϵ''_{SI} scaled by the factor $b_\epsilon \cong \phi_{bI}^{-1}$ for large ϕ_{bI} (Figures 7 and 8), exponential c_{bI} dependence of the characteristic time τ* for large c_{bI} (Figure 9), and the rather weak nonlinearity explained in part 2. These facts indicate that the fast process is attributed to the starlike relaxation of individual I blocks. Quantitatively, τ* for entangled I blocks are 2−3 orders of magnitude longer than the relaxation time for the corresponding star chains. Analyses in terms of the tube model suggest that this difference reflects effects of the impenetrable S cores that constrain the I block relaxation (Figures 10 and 11).

For the slow process of the concentrated micelles entangled through their corona I blocks, good agreement is found between the relaxation time τ_s and the Stokes−Einstein (SE) diffusion time τ_{SE}, the latter being evaluated for $\eta_{eff} = \eta_{fast}$ (viscosity for the relaxation of individual I blocks). This result strongly suggests that the slow process of the entangled micelles is attributed to their SE diffusion that is governed by the relaxation of the I blocks. On the other hand, τ_s of dilute SI and SB micelles in *nonentangling* matrices are close to τ_{SE}^{o} evaluated for $\eta_{eff} = \eta_{mat}$ (matrix viscosity), suggesting that the slow process of those dilute micelles is also due to the SE diffusion (in the pure matrices). However, the data for dilute SB micelles in entangling matrices cannot be explained from the SE mechanism. This problem deserves further attention.

References and Notes

(1) Watanabe, H.; Kotaka, T.; Hashimoto, T.; Shibayama, M.; Kawai, H. *J. Rheol.* **1982**, *26*, 153.
(2) Watanabe, H.; Kotaka, T. *Polym. J.* **1982**, *14*, 739.
(3) Watanabe, H.; Kotaka, T. *Polym. J.* **1983**, *15*, 337.
(4) Watanabe, H.; Kotaka, T. *J. Rheol.* **1983**, *27*, 223.
(5) Watanabe, H.; Yamao, S.; Kotaka, T. *J. Soc. Rheol. Jpn.* **1982**, *10*, 143.
(6) Watanabe, H.; Kotaka, T. *Macromolecules* **1983**, *16*, 769.
(7) Watanabe, H.; Kotaka, T. *Macromolecules* **1984**, *17*, 342.
(8) (a) Watanabe, H.; Sato, T.; Osaki, K. *Macromolecules* **1996**, *29*, 104. (b) Watanabe, H.; Sato, T.; Osaki, K. *Macromolecules* **1996**, *29*, 113.
(9) Stockmayer, W. H. *Pure Appl. Chem.* **1967**, *15*, 539.
(10) Yao, M.-L.; Watanabe, H.; Adachi, K.; Kotaka, T. *Macromolecules* **1991**, *24*, 2955.
(11) Yao, M.-L.; Watanabe, H.; Adachi, K.; Kotaka, T. *Macromolecules* **1991**, *24*, 6175.
(12) Yao, M.-L.; Watanabe, H.; Adachi, K.; Kotaka, T. *Macromolecules* **1992**, *25*, 1699.
(13) Watanabe, H. *Macromolecules* **1995**, *28*, 5006.
(14) Osaki, K.; Nishizawa, K.; Kurata, M. *Macromolecules* **1982**, *15*, 1068.
(15) Osaki, K.; Takatori, E.; Kurata, M.; Watanabe, H.; Yoshida, H.; Kotaka, T. *Macromolecules* **1990**, *23*, 4392.
(16) Osaki, K. *Rheol. Acta* **1993**, *32*, 429 and references therein.
(17) Menezes, E. V.; Graessley, W. W. *J. Polym. Sci., Polym. Phys. Ed.* **1982**, *20*, 1817.
(18) Watanabe, H.; Sato, T.; Osaki, K.; Yao, M.-L. *Macromolecules* **1996**, *29*, 3890 (following paper in this issue).
(19) Fujimoto, T.; Nagasawa, M. *Advanced Techniques for Polymer Synthesis*; Kagaku-Dojin: Kyoto, 1972.
(20) Adachi, K.; Kotaka, T. *Prog. Polym. Sci.* **1993**, *18*, 585 and references therein.
(21) Yoshida, H.; Adachi, K.; Watanabe, H.; Kotaka, T. *Polym. J.* **1989**, *21*, 863.
(22) Adachi, K.; Yoshida, H.; Fukui, F.; Kotaka, T. *Macromolecules* **1990**, *23*, 3138.
(23) Watanabe, H.; Urakawa, O.; Kotaka, T. *Macromolecules* **1993**, *26*, 5073; **1994**, *27*, 3525.
(24) Raju, V. R.; Menezes, E. V.; Marin, G.; Graessley, W. W.; Fetters, L. J. *Macromolecules* **1981**, *14*, 1668.
(25) Watanabe, H.; Kotaka, T. *Chemtracts: Macromol. Chem.* **1991**, *2*, 139 and references therein.
(26) Watanabe, H.; Yamazaki, M.; Yoshida, H.; Kotaka, T. *Macromolecules* **1991**, *24*, 5573.
(27) Fetters, L. J.; Kiss, A. D.; Pearson, D. S.; Quack, G. F.; Vitus, F. J. *Macromolecules* **1993**, *26*, 647.
(28) Pearson, D. S.; Helfand, E. *Macromolecules* **1984**, *17*, 888.
(29) Doi, M.; Kuzuu, N. *J. Polym. Sci., Polym. Lett. Ed.* **1980**, *18*, 775.
(30) Doi, M.; Edwards, S. F. *The Theory of Polymer Dynamics*; Clarendon: Oxford, U.K., 1986.
(31) Dimarzio, E. A. *J. Chem. Phys.* **1965**, *42*, 2101.
(32) Tsunashima, Y.; Hirata, N.; Nemoto, N.; Kurata, M. *Macromolecules* **1988**, *21*, 1107.

MA951843R